Scale-up Considerations of the Sundial Rotating Fresnel Solar Collector

Mercedes Ibarra [1[https://orcid.org/0000-0001-9859-2435]], Rubén Barbero [1[https://orcid.org/0000-0002-6033-1309]], Magdalena Barnetche [2[https://orcid.org/0000-0001-7263-2224]], Rubén Abbas [2[https://orcid.org/0000-0003-3948-3292]], and Antonio Rovira [1[https://orcid.org/0000-0002-6810-3757]]

[1] Universidad Nacional de Educación a Distancia (UNED), Spain

[2] Universidad Politécnica de Madrid (UPM), Spain

Abstract. In the frame of the ASTEP project two prototypes of the Sundial collector, together with a Phase Change Material Thermal Energy Storage, will be tested integrated with the industrial processes of two sites. However, the size of the pilot systems will not be optimized for commercialization. The present work considers the scale-up of the concept for one of the pilot industrial sites: a dairy industry located in Greece, and how will the thermal losses of the system must be considered with the increased aperture, thermal storage size and energy output. For the scaling up of the system, the capacities of the Sundial, demand and TES were doubled and multiplied by 10, and the thermal losses of both nominal conditions and annual performance were considered. The results showed that the ratio between the piping heat losses and the total available energy decreased when scaling-up the system both in the nominal and in the annual results. Hence, the heat losses lost importance when scaling up, when more energy was available. These facts should be considered when evaluating the performance of the pilots and feasibility of the concept.

Keywords: SHIP, Modelling, Heat Losses

Introduction

Solar concentrating collectors may be used as power source for industrial heat and cooling demands, especially among the medium temperature range (150-300 °C). There are commercial references of systems using both parabolic trough collectors and Fresnel collectors [1], [2]. However, the technology must overcome several challenges, such as the intermittency of the solar resource or the cost of the systems to improve its market development. The European ASTEP (Application of Solar Thermal Energy to Processes) Project, financed by the H2020 program, proposed the use of a rotating Fresnel collector (Sundial) together with a Phase Change Material (PCM) thermal energy storage (TES) to address such challenges.

In the frame of this project two prototypes of the ASTEP concept (consisting of the Sundial collector together with the PCM-TES), will be tested integrated with the industrial processes of two sites. The objetive of the concept is to provide heat and cooling for industrial processes. Previous papers have provided detailed information concerning the design of the pilot collector [3], [4], its optical design and optimization [5], receiver performance [6], [7] and the performance of the collector when integrated with the ASTEP concept. The steady state modelling and results of the whole system were presented in [8], [9] and the dynamic behavior of the Sundial in was presented in [10], focusing on the effects of the thermal inertia of the system in [11].

However, the size of the pilot system has not been optimized for commercialization. The present work considers the scale-up of the concept for one of the pilot industrial sites (a dairy industry located in Corinth, Greece), with the objective of improving the efficiency and reducing the cost. To scale-up it up, some aspects require additional attention. The main one will be the thermal losses of the system and their relationship with the increased aperture, thermal storage size and energy output. Both the heat losses for the nominal conditions and for the annual performance of the system were calculated through the steady state model presented in [8].

Methodology

Description of the system

The ASTEP concept consists of the integration of a Fresnel solar collector, with a PCM-TES, to act as heat and/or cold sources for industrial processes. The solar collector, called Sundial has 47,5 m^2 of aperture area (8 mirrors) and two evacuated tube in series (4 m each) as receiver. The control system ensured an outlet collector temperature of 240ºC as long as there was enough irradiation to reach it [10]. The TES consists of a PCM filled tank where the heat exchange between this material and the heat transfer fluid (HTF) was carried out through a tube that passes through the PCM storage 60 times. Surrounding the tube, a metal cell, optimized for the improvement of the heat exchange between the PCM and the HTF. The energy produced in the solar collector was either accumulated in the TES or sent to the demand. The reference case considered in this paper (shown in Figure 1) was the system designed for a dairy industry located in Corinth (Greece) with heat and cooling demands of 8 kWth and 6 kWth respectively, which has 2 TES modules of 60 cells each according to its optimum design [8].

As previously discussed, the models for the design and evaluation of this concept were already presented by [8]. In this paper, the focus will be on the scale-up of the concept and its effect on the heat losses. To do so, the pipes connecting the different elements were identified, and their length and working temperature and flowrate were determined. Figure 1 shows the identification of each pipe segment considered.
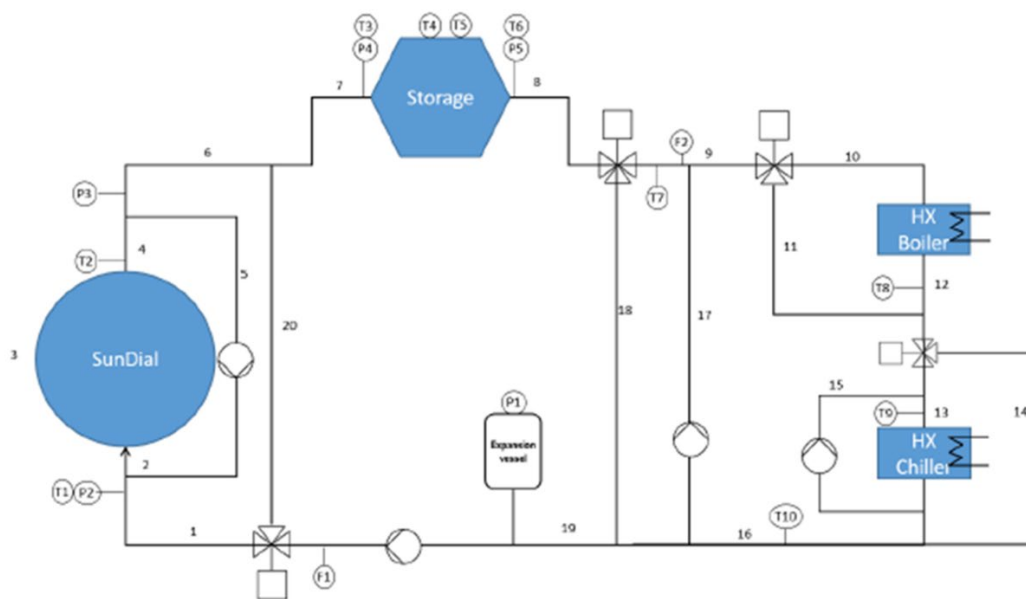

Figure 1. Scheme of the reference case: ASTEP concept for an industry with heat and cooling demands.

Heat Losses Calculations

The dimensions of the pipes were determined by ensuring a fluid velocity of 0,1 m/s and pressure losses below 0,4 bar per pipe segment. Four layers are considered (see Figure 2): the inside of the pipe, where the HTF circulates, the steel pipe, the isolation (mineral wool) and the external air.
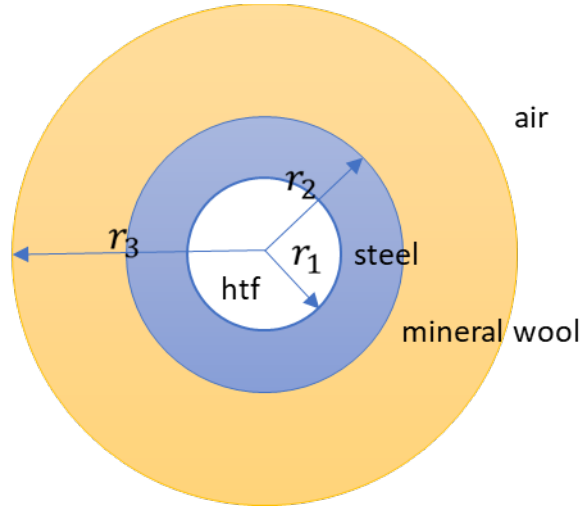

Figure 2. Cross-cut scheme of the layers considered in the pipes.

The heat losses per meter (Q_{HL}) were calculated for every segment of pipes based on the dimensions of the pipes and the heat transfer coefficients of the air, heat transfer fluid and materials of the pipe (see below), based on Barnetche et al. [11]:

$$Q_{HL} = \frac{1}{h_{htf}2\pi r_1} + \frac{ln(r_2/r_1)}{2\pi k_s} + \frac{ln(r_3/r_2)}{2\pi k_{mw}} + \frac{1}{h_0 2\pi r_3}$$

(1)

Where r_1, r_2 and r_3 were the ratio of the corresponding layer, k_s was the thermal conductivity of the steel, k_{mw} was the thermal conductivity of the mineral wool and h_i was the heat losses coefficient, calculated by:

$$h_i = \frac{Nu_i \cdot k_i}{2 \cdot r_i}$$

(2)

where k_i was the thermal conductivity of the element (air or HTF) and *Nu* was the Nusselt number, calculated using the using the Dittus-Boelter equation [12]. The values of theses parameters are found in Table 1.

Table 1. Parameters for the heat losses calculations

Parameter	Value
Thermal conductivity of the steel (k_s)	45,5 W/m·K
Thermal conductivity of the mineral wool (k_{mw})	0,042 W/m·K
Thermal conductivity of the air (k_{air})	$26,3 \times 10^{-3}$ W/m·K
Thermal conductivity of the heat transfer fluid (k_{htf})	$99,3 \times 10^{-3}$ W/m·K
Ambient temperature (T_{amb})	20 °C
Air velocity (v_{air})	0,1 m/s

Therminol 59 was used as heat transfer fluid in the system. The properties of the oil are temperature dependent, and the polynomial equations to evaluate these properties were adjusted from [13] (with T in °C) as follows:

Density

$$\rho = -0,7996 \cdot T + 997,87 [kg/m^3]$$

(3)

Heat capacity

$$c_p = (0,003383 \cdot T + 1,5991) \cdot 1000 [J/kg \cdot K]$$

(4)

Thermal conductivity

$$k = -0,000119 \cdot T + 0,128 [W/m \cdot K]$$

(5)

Viscosity

$$\mu = -(0,00000000095681 \cdot T^4 - 0,00000093791 \cdot T^3 + 0,00035429 \cdot T^2 - 0,063367 \cdot T^4 + 4,9521) \cdot 0,001 [Pa \cdot s]$$

(6)

System Scaling-Up

For the scaling up of the system, the capacities of the Sundial, demand and TES were doubled and multiplied by 10, and the dimensions of the pipes were adjusted accordingly (see Table 2). Both the heat losses on design and within the yearly simulations were calculated through a steady state model presented in [8].

Table 2. Characteristics of the segments of the pipes for the ASTEP.

Pipe Segment	Length (m)	T_{htf} (°C)	DN Ref	DN x2	DN x10
1	14	224	20	36	65
2	2	237	40	80	200
3	5	237	40	80	200
4	2	240	40	80	200
5	5	240	40	80	200
6	13	240	20	36	65
7	4	240	20	36	65
8	4	235	20	36	65
9	2	205	20	36	65
10	1	205	20	36	65
11	2	205	20	36	65
12	1	205	20	36	65
13	2	190	20	36	65
14	2	190	20	36	65
15	2	95	20	36	65
16	2	90	20	36	65
17	2	180	20	36	65
18	2	235	20	36	65
19	4	224	20	36	65
20	2	224	20	36	65

Results and Discussions

The heat losses of the piping were calculated for three sizes of the ASTEP concept, both in nominal conditions and through a whole year. Table 3 shows the results of the heat losses per meter in each pipe segment. As expected, within one design (ref, x2 or x10) the pipes with greater size have more thermal losses per meter. Moreover, when scaling-up the designs, the increased dimensions of the scaled-up pipes meant an increase of the thermal losses per meter ($Q_{HL,dis}$), as seen in Table 3.

Table 3. Heat losses of the segments of the pipes for the ASTEP.

Pipe Segment	$Q_{HL,dis}$ Ref (W/m)	$Q_{HL,dis}$ x2 (W/m)	$Q_{HL,dis}$ x10 (W/m)
1	22,24	23,22	25,01
2	25,24	26,98	28,64
3	25,24	26,98	28,64
4	25,64	27,41	29,10
5	25,62	27,39	29,09
6	24,04	25,10	27,03
7	24,04	25,10	27,03
8	23,49	24,53	26,42
9	19,85	23,10	23,79
10	20,00	23,29	23,91
11	0,00	0,00	0,00
12	20,00	23,29	23,91
13	18,43	21,47	20,73
14	18,31	21,32	21,90
15	7,24	8,44	8,65
16	7,25	8,44	8,66
17	17,04	19,84	20,42
18	23,46	27,33	26,40
19	22,24	23,22	25,01
20	0,00	0,00	0,00

The analysis of the results of the whole system (taking into account the actual lengths) in the nominal and annual results are shown in Figures 3 and 4. These figures show the ratio between the sum of the piping heat losses and the total available energy (the one delivered by the boiler and chiller). The ratio decreased when scaling-up the system for both in the nominal results (Figure 3 a), where the ratio of the powers is shown) and in the annual ones (Figure 3 b), where the ratio is for the energies). These decreases went from 0,1116 (in the reference case) to 0,0127 (in the x10 scale-up case) for the nominal conditions, and from 0,1854 to 0,0122 for the yearly simulations. The ratio of heat losses was higher for the reference and the x2 scale-up cases, meaning that the heat losses on the nominal conditions were underrepresented when compared with the performance in other conditions along the year. However, the differences among the nominal and the yearly results for the x10 scale-up case were smaller (and the ratio was higher in the nominal conditions), meaning that the heat losses in the nominal conditions when scaling up would represent the heat losses to be expected along the year.
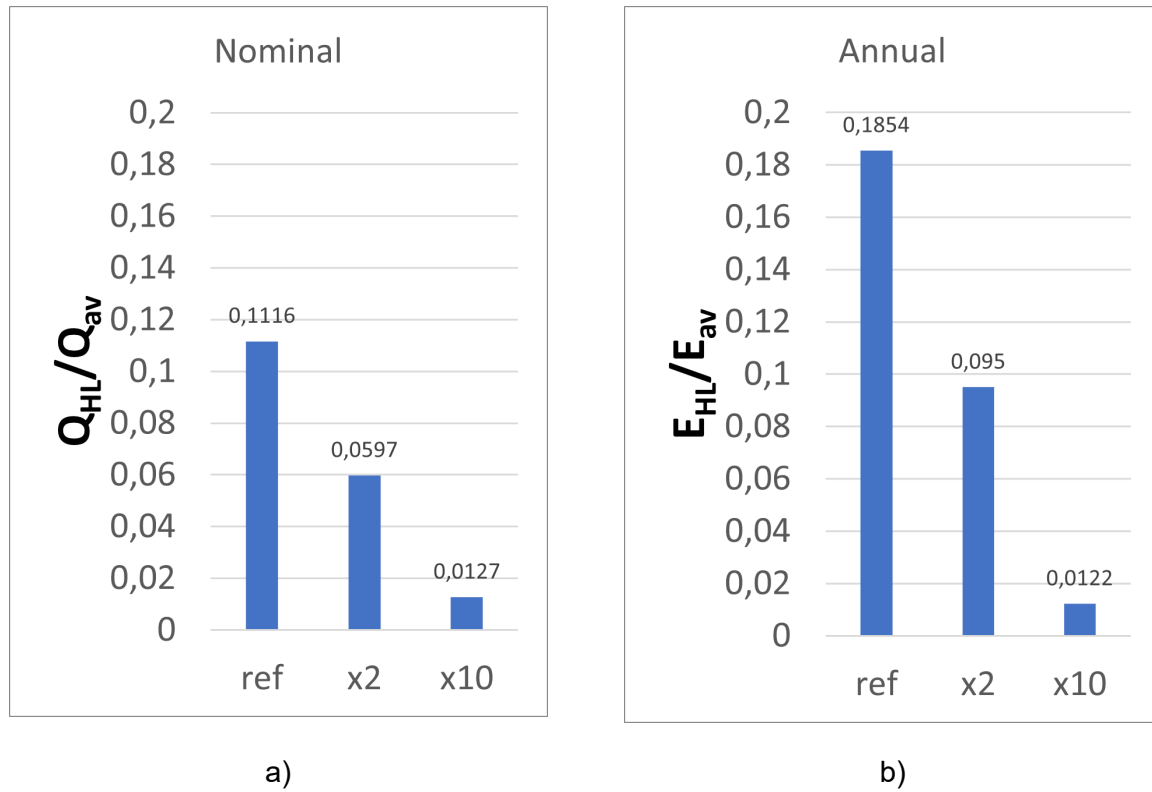
a)   b)

Figure 3. a) Ratio of the thermal losses (kW) and the available power (kW) for the three scales for the nominal conditions and b) ratio of the thermal losses (kWh) and the available energy (kWh) in the annual results for the three scales

Figure 4 shows this same ratio along the year, for each month. The ratio of heat losses thought the year was also less important during the summer months (April to September), when more energy is available.
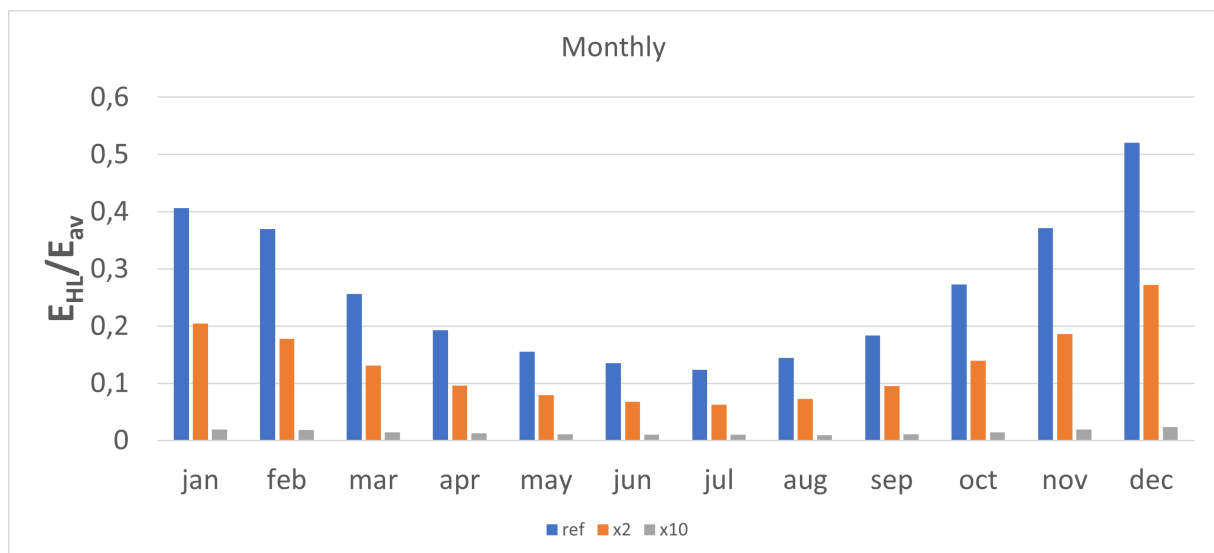

Figure 4. Monthly ratio of the thermal losses (kWh) and the available energy (kWh) or the three scales.

Conclusions

The heat losses associated to a pilot SHIP system to be installed were evaluated for the design and for the scale-up of the concept. As expected, the pipes with greater size have more thermal losses per meter. When scaling-up the designs, the increased dimensions of the scaled-up pipes meant an increase of the thermal losses per meter.

However, the ratio between the piping heat losses and the total available energy (the produced one produced by the boiler and chiller) decreased when scaling-up the system, when more energy was available. This behavior was reflected both in the nominal conditions and in the yearly results. The ratio of heat losses thought the year were also less important during the summer months.

Hence, the heat losses lost importance when scaling up, as more energy was available, and the percentage that the heat losses represented decreased. These facts should be considered when evaluating the performance of the pilot and feasibility of the ASTEP concept, as the heat losses in the pilot may be of significance.

Author contributions

Mercedes Ibarra: Conceptualization, Methodology, Software, Writing-Original Draft, Visualization. **Rubén Barbero:** Conceptualization, Writing-Review and Editing**. Magdalena Barnetche**: Methodology, Writing-Review and Editing. **Rubén Abbas**: Writing-Review and Editing. **Antonio Rovira**: Writing-Review and Editing.

Competing interests

The authors declare no competing interests

Funding

References

[1] "Home | Solar Heat for Industrial Processes (SHIP) Plants Database." http://ship-plants.info/ (accessed Sep. 30, 2022).

[2] D. R. Krüger, B. Epp, T. Hirsch, and J. Stengler, "Status in Solar Heat from Concentrating Solar Systems," 2022.

[3] J. Cano-Nogueras, J. Muñoz-Antón, and J. M. Martinez-Val, "A New Thermal-Solar Field Configuration: The Rotatory Fresnel Collector or Sundial," *Energies*, vol. 14, no. 14, p. 4139, Jul. 2021, doi: https://doi.org/10.3390/en14144139.

[4] A. Sebastián, R. Abbas, M. Valdés, and A. Rovira, "Modular micro-trigeneration system for a novel rotatory solar Fresnel collector: A design space analysis," *Energy Convers. Manag.*, vol. 227, p. 113599, Jan. 2021, doi: https://doi.org/10.1016/j.enconman.2020.113599.

[5] R. Abbas *et al.*, "Enhancement of SunDial optical performance handling cosine and end losses," in *AIP Conference Proceedings*, Freiburg, Germany, May 2022, vol. 2445, p. 140001. doi: https://doi.org/10.1063/5.0085667.

[6] R. Barbero *et al.*, "Thermal losses characterization for the receiver of the SunDial, the rotary Fresnel collector," presented at the SolarPACES 2021, Sep. 2021. doi: https://doi.org/10.5281/zenodo.5772950.

[7] M. J. Montes, R. Abbas, R. Barbero, and A. Rovira, "A new design of multi-tube receiver for Fresnel technology to increase the thermal performance," *Appl. Therm. Eng.*, vol. 204, p. 117970, Mar. 2022, doi: https://doi.org/10.1016/j.applthermaleng.2021.117970.

[8] M. Ibarra, R. Barbero, M. Barnetche, L. F. Gonzalez-Portillo, R. Abbas, and A. Rovira, "Design and integration of a solar heat system based on the SunDial for industrial processes," presented at the SolarPACES 2021, Sep. 2021. doi: https://doi.org/10.5281/zenodo.5772878.

[9] M. Ibarra *et al.*, "Dateset of results: yearly operation for AMTP and MAND - steady state simulation (D3.3 D5.1)." Jan. 28, 2022. doi: https://doi.org/10.5281/zenodo.5914138.

[10] M. Barnetche, L. F. González-Portillo, M. Ibarra, R. Barbero, A. Rovira, and R. Abbas, "Dynamic analysis of the SunDial, the rotatory Fresnel collector," presented at the SolarPACES 2021, Sep. 2021. doi: https://doi.org/10.5281/zenodo.5772923.

[11] M. Barnetche *et al.*, "Analysis of the thermal inertia of pipelines in SHIP," presented at the XII National and III International Conference on Engineering Thermodynamics, Madrid, Spain, Jun. 2022.

[12] F. P. Incropera, *Fundamentals of heat and mass transfer*, 3rd ed. Chichester [etc.]: John Wiley and Sons, 1990.

[13] "Therminol 59 Technical Datasheet." Eastman Corporate, 2020. Accessed: Oct. 04, 2022. [Online]. Available: https://www.eastman.com/Literature_Center/T/TF9029.pdf